

Can Binary Bound States in a Strongly Coupled Quark-Gluon Plasma be observed via dileptons and photons?

Jorge Casalderrey-Solana and Edward V. Shuryak
Department of Physics and Astronomy
State University of New York, Stony Brook, NY 11794-3800
 (November 13, 2018)

Recently there was a significant change of views on physical properties and underlying dynamics of Quark-Gluon Plasma at $T = 170 - 350 \text{ MeV}$, produced in heavy ion collisions at RHIC. Instead of weakly coupled gas of quasiparticles, it is rather a liquid-like matter with multiple bound states. In this paper we discuss how one can test these ideas experimentally, using the “penetrating probes” and looking for certain peaks at some invariant masses. In dileptons the most promising are modified ρ, ω , with $M(T \approx T_c) \sim .5 \text{ GeV}$ and also near zero binding at $M(T \approx (1.5 - 2)T_c) = 1.5 - 2 \text{ GeV}$. We also discuss the observability of peaks corresponding to scalar/pseudoscalar mesons in the two-photon channel.

I. INTRODUCTION

A. The penetrating probes

To use photons and dileptons as “penetrating probes” to study the earlier stages of heavy ion collisions was one of the first suggestions to study quark-gluon plasma (QGP) [1]. Although these particles are produced much less copiously compared to hadrons, and thus they are more difficult to study, photons and leptons are of special importance because they do not suffer final state interaction and therefore can bring us direct information about the earliest (the hottest) stages of the collision. In this respect one may compare them to e.g. solar neutrinos, which bring direct information about the conditions at Sun’s interior.

It was argued in [1] that because of the QCD phase transition, one should expect the invariant mass ($M^2 = (p_{l+} + p_{l-})^2$) spectra of penetrating probes produced in QGP to be qualitatively different from those originating in hadronic matter. However only monotonously decreasing mass spectra were expected from QGP, in contrast to familiar vector meson $\rho, \omega, \phi, J/\psi \dots$ peaks from the hadronic phase. The rates were calculated in a picture of weakly interacting and freely moving near-massless quark quasiparticles, below wQGP for brevity.

Recently a radically new picture of QGP has been developed, to be described in next subsection, based on much stronger coupling between quasiparticles, to be referred to as sQGP. One aspect of it is that the meson-like bound states continue to exist at $T = (1 - 2)T_c = 170 - 350 \text{ MeV}$ (the temperature range corresponding to QGP at RHIC), although in a strongly modified form. Furthermore, even at higher T when there are no bound states, there exist near-threshold enhancement which may still be used to infer the value of the quasiparticle masses and the strength of their interaction.

As penetrating probes are emitted during the whole expansion of the fireball, the evaluation of observable spectra includes two very different steps. (i) First one evaluates a *production rate* in equilibrium matter at a given

T , $dR(T)/d^4x d^4q$ per time per volume per 4-momentum. The second step (ii) is the space-time integration over the 4-volume of the expanding fireball, from its creation to final freezeout. At the first step (i) there will be certain peaks at fixed values of mesons masses, but since they are in general T -dependent, $m_V(T)$, the time integral at the second step will in general smoothen them out. Only peaks corresponding to special points can survive and be observable, as we detail below.

Let us start with the basic expression for the dilepton production rate

$$\frac{dR(T)}{d^4x d^4q} = \frac{\alpha^2}{48\pi^4} \frac{1}{e^{\frac{q_0}{T}} - 1} F \quad (1)$$

where α is the electromagnetic coupling, q_0 is the dilepton energy and the “formfactor” F for two well-tested processes are,

$$F = \begin{cases} F_H \stackrel{\text{def}}{=} \frac{m_\rho^4}{[(m_\rho^2 - M^2)^2 + m_\rho^2 \Gamma_\rho^2]}, & (\rho) \\ F_Q \stackrel{\text{def}}{=} 12 \sum_q e_q^2 \left(1 + \frac{2m_q^2}{M^2}\right) \left(1 - \frac{4m_q^2}{M^2}\right)^{\frac{1}{2}}, & (wQGP) \end{cases} \quad (2)$$

where the former one corresponds to $\pi\pi \rightarrow \rho \rightarrow l^+l^-$ annihilation in a vacuum or hadronic phase at small T , written in standard vector-dominance form. The latter expression corresponds to $\bar{q}q$ annihilation similar to partonic Drell-Yan process. If one ignores quark masses in F_Q , it is just a sum of squared charges for all relevant quarks, u, d, s of all colors. This basic case we will use as our “standard candle” below, normalizing all predictions to the “standard wQGP rate” with $F_{wQGP} = 24$. Detailed calculation of the final dilepton spectra for such “standard candle” model were done by Rapp and Shuryak [2] (including specific acceptance of the SPS NA50 experiment) and for RHIC by Rapp [4]. For a review see [5].

In terms of the imaginary part of the photon self energy wQGP limit means

$$\Im \Pi_{em} = -\frac{M^2}{12\pi} N_c \sum_{q=u,d,s} (e_q^2) \quad (3)$$

If quark quasiparticles in the QGP phase are not massless (and current lattice calculations indicate they are as heavy as 1 GeV in the region of interest $T_c - 3T_c$) one would like to correct for that using the formulae from above. This fact leads to a trivial modification to the previous expression (that is relevant in the IMR)

$$\Im\Pi = \begin{cases} 0, & (M^2 < 4m_q^2) \\ \frac{-M^2}{12\pi} N_c \sum_q e_q^2 \left(1 + \frac{2m_q^2}{M^2}\right) \left(1 - \frac{4m_q^2}{M^2}\right)^{\frac{1}{2}}, & (M^2 > 4m_q^2) \end{cases}, \quad (4)$$

Furthermore, we expect nontrivial modification of the annihilation cross section of quarks into leptons due to the attractive interaction between them. This modification will be specially important for near threshold production, where we will use non relativistic Green's functions. Modifications of the rates are also expected due to the presence of bound states, where, as we will see, the problem is intrinsically relativistic.

Dileptons produced by vector resonances ($\rho, \omega, \phi, J/\psi$) are described by the first expression in (2), which can be used both in a hadronic phase and in sQGP. There exist large literature on matter-induced modification of mesons in hadronic phase. For sufficiently dilute matter one can use linear density approximation, in which the modification of real and imaginary part (the mass and the width) of a state is simply determined by forward scattering amplitudes *in vacuum* which are often experimentally known. For example, $\pi\rho$ and $N\rho$ scattering used in [7] are mostly responsible for modification of ρ resonance. Quite a number of works following such ideas found relatively modest shifts of resonance masses (e.g. m_ρ) downward and some broadening*. Further assumptions are needed when the matter is not dilute: e.g. the Li-Ko-Brown model [6] assumed that all hadronic masses are shifted proportional to Walecka-type scalar mean field, related to local matter density. As example of self-consistent approach see e.g. a set of coupled gap equations discussed by Rapp and Wambach [5]: it predicted very strong broadening of the ρ meson due to mixing between ρ with excitations of the lowest baryon resonances, such as[†] $N^*(1520)N^{-1}$.

Let us now proceed to a brief review of dilepton experiments. Since these kind of measurements are generally much more difficult to do (there are large background to be rejected, while the process itself has small cross section), they have a sad tendency to come "too late", right before the program gets closed.

*As shown in [8], mass reduction leads to some suppression of the decay, which often tends to cancel widening from a rescattering. This was experimentally confirmed by STAR experiment at RHIC [9], which found no width change of the ρ observed via $\pi\pi$ at late stages.

[†]This notation means a nucleon excited into a baryonic resonance by vector meson absorption.

At Berkeley BEVALAC the DLS dilepton spectrometer has found a spectacular effect, but the detector efficiencies were debated years after its last run[‡]. Brookhaven AGS program had no dilepton experiments, while CERN SPS program included: (i) CERES (NA45), which studied the low mass ($M=0-1$ GeV) e^+e^- pairs, (ii) HELIOS-3, which studied medium mass $\mu^+\mu^-$ $M=1-2$ GeV, and (iii) NA38/50/60 concentrated on $\mu^+\mu^-$ with $M=2-4$ GeV. All of them observed quite significant enhancement over "standard hadronic sources", ranging from factor 5 at CERES (in some kinematic region) to about 3 at NA38/50 for intermediate masses $M=2-3$ GeV. The observed effective " ρ melting" at CERES and thermal continuum at NA50 indicates an approach toward chiral symmetry restoration and QGP [2,3]. This is quite puzzling, since at the SPS only a small fraction of the space-time volume contributing to dilepton production is expected to originate from QGP, while most of it should still be from the mixed or hadronic phase. The NA50 experiment now evolved into NA60 which is supposed to resolve the remaining uncertainty between thermal dileptons and charm contribution, as well as significantly increase mass resolution and tell us about possible modifications of narrow ω, ϕ resonances.

The dileptons are supposed to be the main part of the RHIC program: PHENIX was aimed at that from the beginning and now also STAR detector has electromagnetic calorimeter. Large-statistics Run-4 data are now being analyzed, and the only published data so far are PHENIX single electron production [10], which is presumably dominated by charm decays.

Matter modification of more narrow ω, ϕ resonances can obviously be observed only for a fraction of these particles decaying inside the fireball. Resonances decaying after freezeout have the usual vacuum mass, and these decays produce large "hadronic background" for such measurements: in fact so far none of the existing dilepton experiments had sufficient resolution to observe these modifications. However for sQGP vector mesons the mass modification is very large, e.g. we will discuss below peaks with masses up to $M \sim 2\text{ GeV}$, and so in this case the resolution is not so much an issue.

In principle, the $\gamma\gamma$ channel of the decays provides another window into early-time spectroscopy, as photons are penetrating probes as well. Still, not much discussion of those can be found in literature. In-matter modification of the *pseudoscalars* π, η are expected to be quite small, as these masses are protected by chiral symmetry and are not expected to be modified much in all hadronic phase $T < T_c$. The experimental observability of these

[‡]There are no official publication yet, but preliminary results from HADES experiment at GSI recently reported have not confirmed this effect in its first run.

[§]At high masses region, $M > 3\text{ GeV}$, the dilepton production is well described by simple partonic Drell-Yan process.

shifts in $\gamma\gamma$ channel is next to impossible, due to huge background from similar decays after freezeout. Scalars and tensors are considered to be too wide even in matter, to get any meaningful signal even before in-matter modification.

The situation again should be quite different for π^0, η, η' and scalars originating from sQGP**, since very large mass shifts are expected. We return to their discussion in section IV below.

B. Bound states in QGP and the penetrating probes

The quark-gluon plasma (QGP) was defined as a state of matter in which a color charge is screened [1] rather than confined. According to lattice and experimental results it takes place above the critical temperature $T_c \approx 170 \text{ MeV}$.

At high temperatures $T \gg T_c$ it should be a gas of weakly interacting quasiparticles (modulo long-range magnetism), wQGP. However a physical picture of QGP structure at not-too-high T , in the temperature range $(1 - 3)T_c$, recently underwent a radical change [11]. The interaction seems to be sufficiently strong to produce multiple bound states of quark and gluon quasiparticles, and we will refer to such matter as strongly coupled QGP (sQGP for brevity).

Using lattice-based potentials, it was shown [12,13] that a picture of binary bound states may provides a consistent description of several previously disconnected lattice observations, such as (i) bound states for charmonium and some light $\bar{q}q$ states [14]; (ii) static potentials [15]; (iii) quasiparticle masses [16]; and (iv) bulk thermodynamics [17]. However more complicated structure can also be present, perhaps in line with a liquid-like behavior needed to understand robust collective flow phenomena at RHIC, well described by ideal hydrodynamics.

Studies of strong coupling and related binary states are also under way in other fields of physics. In particular, the $\mathcal{N}=4$ supersymmetric Yang-Mills theory at finite T is a perfect toy model, in which a parametric transition from weak to strong coupling can be traced, see discussion of binary states in [18]. Another strongly-coupled system is produced experimentally, by cold trapped atomic gases, by tuning the scattering length to very large values via Feshbach resonances. Hydro-type flow and small damping of oscillations observed for these systems indicate liquid-like properties of matter in this case as well [19].

The goal of this paper is to formulate how one can tell the difference between the wQGP (with light and

weakly interacting quarks) from the sQGP picture outlined above, by using a dilepton penetrating probe. More specifically, we will discuss the following questions:

- (i) Is it possible to measure the interaction between quark quasiparticles directly, using the dilepton probe?
- (ii) Where are the most significant differences between sQGP and wQGP scenarios, in respect to the dilepton production?
- (iii) How large are they and whether one has a chance to observe them, at RHIC and elsewhere?

We identify two such mass regions:

- (i) $M \sim 1.5 - 2 \text{ GeV}$ corresponding to $T \approx T(\text{zero binding})$ and the edge of the quasiparticle continuum, at the initial QGP at RHIC.
- (ii) $M \sim 0.5 \text{ GeV}$, where we expect to see the contributions of the modified vector mesons at $T \approx T_c$.

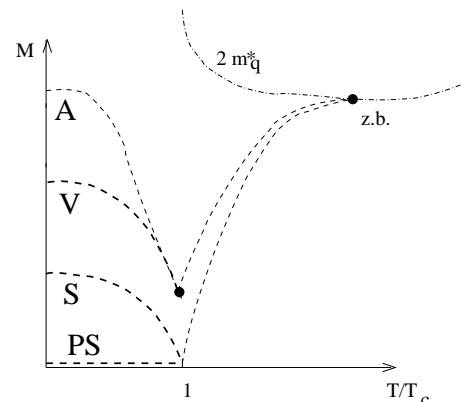


FIG. 1. Schematic T -dependence of the masses of $\bar{q}q$ states. A, V, S and PS stand for axial, vector, scalar and pseudoscalar states. The dash-dotted line shows a behavior of twice the quasiparticle mass. Two black dots indicate places where we hope the dilepton signal may be observable.

The basic idea is very simple: the probability of $\bar{q}q \rightarrow l^+l^-$ process is enhanced by the initial state attractive interaction. Attractive interaction obviously correlate \bar{q} and q in space and increases the chances to find $\bar{q}q$ close to each other and annihilate. In such general form, the enhancement persists whether the potential is deep enough to make bound levels or not, and whether quark quasiparticles have small or large width.

In the case of pure Coulomb interaction this phenomenon is well studied. The relevant parameter $z = \pi\alpha/v$ contains the ratio of the coupling strength to velocity, and the enhancement is in this case given by the well known Gamow factor^{††}

$$F_{\text{Gamow}} = \frac{z}{1 - \exp(-z)}. \quad (5)$$

**We thank V.Zakharov who suggested it to one of us (ES) as a possibility, in a discussion after his talk.

^{††}The sign in exponent is the opposite to that on the original Gamow factor, for alpha-particle interaction with nuclei or that used for HBT correlations, corresponded to a *repulsive* Coulomb force.

Note that the result is $\sim 1/v$ at small v (large z) and 1 at small z . It cancels the velocity in the phase space and makes the production rate to jump to a *finite* value at the threshold.

A good example of the QCD-based color-Coulomb enhancement is the cross section for the production of the top quark pair $t\bar{t}$, see [20,21]. The enhancement calculated in these works is found to be quite significant, in spite of the fact that rather large width of the top quarks precludes them from forming toponium bound states. We will use methods developed in these works in section IIb.

In section II we will discuss the dilepton production in QCD at $T > T_c$. But before we get to discuss details, let us now point out our main ideas. In Fig.1 (which is a modified version of a figure present already in [11] we show schematic temperature dependence of lowest $\bar{q}q$ states. Dileptons can only come from colorless vector pairs (marked by V).

New (sQGP) part of this picture is at $T > T_c$, which starts and ends at points marked by small black circles. At any given T there are two peaks in the spectral density, corresponding to invariant masses of T, L components. On top of that, there is a threshold bump at $2m_q^*(T)$, which exists even at T so high that no bound states exists. Unfortunately, one can only observe a signal integrated over the expanding fireball, or over all temperatures involved between the initial and freezeout ones. The integral tends to wipe out peaks at intermediate locations, unless there are special reasons for them to survive. Two of the black dots, at the mixed phase $T = T_c$, have a benefit of long time spent there during expansion. The same is true for the third black point, due to near-constancy of the mass of weakly bound states at $T = 1.5 - 2T_c$. The near-threshold bump is at about the same location at higher T as well. Thus one may hope (and we will show it below) that the structures corresponding to these endpoints (black circles at Fig.1) may be detected.

Although at finite temperatures and non-zero momentum relative to heat bath are split into distinct longitudinal and transverse (L, T) modes, those should coincide at zero momentum. Since all masses are large compared to relevant T at the time, only pairs with small momentum are actually produced. Furthermore, lattice experience of similar quasiparticle modes indicate that they follow, at least approximately, the vacuum-like dispersion law $\omega^2 = p^2 + M^2$, and so using the invariant mass rather than energy would take care of canceling the momentum dependence.

In Fig.1 we have shown only states made of u, d quarks, ignoring the strange one. Needless to say, those exist and can be also produced. The peaks of $\bar{s}s$ ϕ -like states should be shifted in mass upward by $2m_s \approx 250 - 300 \text{ MeV}$, but their contribution to dilepton spectra is proportional to square of the electric charge $q_s^2 = 1/9$, which is 3 times smaller than the average of $q_u^2 = 4/9, q_d^2 = 1/9$. Strange states are more promising

for pseudoscalar/scalar signals to which we turn below.

II. GENERALITIES

A. From annihilation rates to the observed dilepton spectrum

Before we proceed to realistic rates, based on lattice-based quasiparticle interaction, let us explain few important points by using a much simpler model.

As explained above, we expect certain structures (“bumps”) to exist in the annihilation rate, related to bound states as well as near-threshold enhancement. Their exact shape is determined both by the interaction between the annihilating quarks (to be studied in detail in this work) as well as the interaction with surrounding matter. The latter leads to a “width” which we will leave to be studied later elsewhere.

Because of this, it is instructive first to show how sensitive is the resulting shape of the observable structures to such widths. Let us illustrate the point by the following example. As a representative of a (near-threshold) bump we start with the rate in which the “formfactor” $F(2)$ is written as

$$F_{bump}/24 = M_0 \frac{e^{-\frac{(M-M_0)^2}{2\Gamma^2}}}{(2\pi)^{1/2}\Gamma} + \frac{1}{\exp[-2 * (M - M_0)] + 1} \quad (6)$$

In Fig.2(a) one can see three examples of such bumps, with different widths Γ .

Although the width is different, the integral over the bump is kept the same. Furthermore, this integral is normalized to “missing” strength of the spectral density due to absent annihilation rate between $M = 0$ and $M = M_0$ (see the second term). We did so because one has to be consistent with the so called *quark-hadron duality*, leading to conservation of the total area of the spectral density. Provided that one is using a sufficiently simple ansatz^{††}, as we do now, the duality restriction provides a valuable relation between the bump strength and the position of the threshold $M_0 = 2M_q$.

(Discussion of this and higher order duality relations in vacuum correlators can be found in the classic paper on the QCD sum rules [22], for more general discussion of duality see [23] and for finite T analogs of it as well as Weinberg-like sum rules see [24].)

Here comes the main point we want to make in this section. Although three bumps in Fig.2(a) look very different, those are for fixed T . In experiment we have to integrate the rate over the expanding fireball: let us see how these bumps will look after it is done.

^{††}Otherwise just one sum rules does not have a predictive power, as experience of QCD sum rules had shown.

Although the space-time evolution of the QGP phase at RHIC is complicated hydro explosion, here and below we will compare with the prediction for RHIC using the same parameterization as used by Rapp in [4], concentrating only in the QGP and mixed phase. The physical basis for such simplification is that the invariant mass of the dileptons is the same in all frames, and therefore motion of the matter can be ignored. (It would not be possible if e.g. one wants to calculate the transverse momentum of dileptons, or other non-invariant property.)

We sketch few details here for completeness. The thermal rate is convoluted with the space time history by

$$\frac{dN_{l+l-}^{thermal}}{dM} = \int_{\tau_0}^{\tau_f} d\tau V(\tau) \int d^3q \frac{M}{q_0} \frac{dR_{l+l-}^{thermal}}{d^4q} \quad (7)$$

The t -dependent volume is modeled as expanding cylinder

$$V(\tau) = (z_0 + v_z t) \pi (r_0 + \frac{1}{2} a_{\perp} t^2)^2 \quad (8)$$

where $r_0 = 6.5 fm$ is the initial transverse overlap, $z_0 = 0.6$ the initial longitudinal length, $v_z = 1.4c$ is the relative longitudinal expansion velocity of the fireball edges and $a_{\perp} = 0.035c^2/fm$ is such that at typical freeze-out time $t_f = 15 - 20 fm/c$ we get a final transverse velocity $v_{\perp} = 0.6c$. The initial temperature of the system is set to $T = 370 MeV$. The expansion is considered is-entropic with the entropy density of the QGP phase given by

$$s_{QGP} = (16 + 10.5 N_f) \frac{4\pi^2}{90} T^3 \quad (9)$$

This fixes the time dependence of the temperature, leading to the transition at $t \approx 4 fm/c$. The mixed phase takes place between $4 fm/c$ and $9 fm/c$. The fraction of QGP in the plasma phase is also calculated from standard requirement of constant entropy

$$S_{tot}/V(\tau) = s_{QGP}(T_c) f_{QGP} + s_{HG}(T_c) (1 - f_{QGP}) \quad (10)$$

In doing the convolution, one has to define how the parameters of the rate, Γ, M_0 depend on T . The results shown in Fig.2(b) correspond to Γ being independent on T while the mass depending linearly on it, $M_0 = 6T$. One can see from a comparison of the input to output figures that three cases, although still distinct, look much more similar. The reason for that is that we kept the integral over the spectral density constant, conforming to parton-hadron duality. The sensitivity to (unknown) width of the bump is reduced because of the averaging.

The effect of time averaging is maximal in this example because we took a simple linear dependence for threshold $M_0 = 6T$. In reality, the dependence is nonlinear with a minimum (see dash-dotted curve in Fig.1). Although the precise shape and position of zero binding point are not yet known (better lattice results, please...) one may think that real dependence of M_0 on T is weaker and the effect of averaging be less significant.

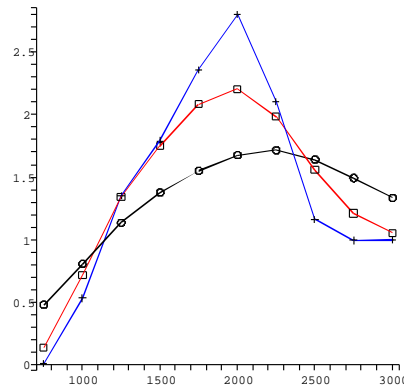
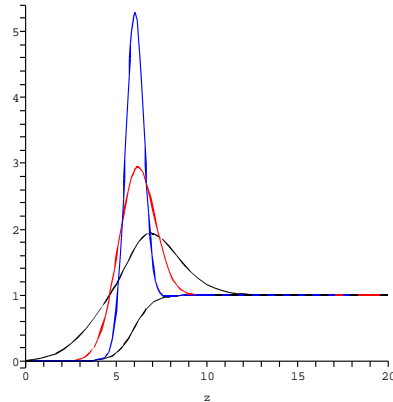


FIG. 2. (a) An example of spectral densities, all of the satisfying the duality condition, *before* time integral. (b) This is how the corresponding spectra look like *after* the averaging over the expanding fireball is performed. The lines marked by crosses, squares and circles correspond to most narrow, the middle and the widest peaks in (a), respectively.

B. Non-relativistic approach and Green functions

As mentioned in the Introduction, the main goal of this paper is to find out how the strong interaction among the initial quarks modifies the dilepton production. Such calculations simplify significantly if one can use the non-relativistic approach. This is clearly possible for invariant masses close to threshold.

The modification is the same in the inverse process, and annihilation of e^+e^- pairs into $q\bar{q}$ has been studied in detail in leptonic colliders. The nonrelativistic methods we use benefit in particular from discussion of Coulomb enhancement of $t\bar{t}$ pairs near threshold in [20], [21].

In [21] the cross section $\sigma(e^+e^- \rightarrow t\bar{t})$ is analyzed to leading-logarithmic order in QCD in the *non relativistic limit* (close to threshold). Their main result, already used in [20], is the modification of the threshold factors from the well known leading order expression

$$\sigma_{LO} = \frac{4\pi\alpha_{QED}^2 e_t^2}{3s} N_c \sqrt{(1 - \frac{4m_t^2}{s})(1 + \frac{2m_t^2}{s})} \quad (11)$$

to

$$\sigma = \frac{4\pi\alpha_{QED}^2 e_t^2}{3s} N_c \frac{24\pi \Im G_{E+i\Gamma_t}(0,0)}{s} \quad (12)$$

Where E is the center of mass energy and Γ_t is the width of the top quark (related to lifetime due to weak decays). The relation for dilepton production rate is obtained by obvious substitution of $\Im G/s$ into F_Q in (2).

As a further clarification, in the limit $\Gamma = 0$ we can rewrite

$$\Im G_{E+i0+}(0,0) = \sum \psi_n(0)\psi_n(0)^\dagger \delta(E_n - E) \quad (13)$$

Note that the sum runs over *all* states, including scattering states, where the sum should be replaced by an integral. This expression explains quite clearly the connection between the Green's function and the standard non relativistic formula for the annihilation of bound states (13) gives the flux factor that multiplies the annihilation cross section at zero momentum

$$\sigma = \sigma_{q\bar{q}}(s = 4m_q)|\psi_n(0)|^2 \quad (14)$$

The non-relativistic Green's function $G_{E+i\Gamma_t}(r, \bar{r})$ obeys the usual Schrodinger equation:

$$[-\frac{1}{m}\vec{\nabla}^2 + V(\vec{r}) - (E + i\Gamma)]G_{E+i\Gamma}(r, \bar{r}) = \delta^3(\vec{r} - \bar{r}) \quad (15)$$

with inter-particle potential $V(\vec{r})$. Analytic expressions for Green's function for the pure Coulomb potential are well known, see e.g. [20]. For realistic lattice-based potential we will use a numerical method following [21], which is valid for all potentials less singular than $1/r^2$. The benefit of it is that one avoid summations over levels, and bound states are automatically included together with scattering ones. As a test, we checked that it reproduces well known results for Coulomb potential with accuracy at least few per mill.

The Green's function, thus, contains, at the non relativistic level, all the information needed about the states of the two particle system. This is important because we are interested not only in bound states but also in modification of scattering states, especially close to zero energy, to be responsible for the threshold effects we will study. The cross section of $q + \bar{q} \rightarrow e^+ + e^-$ is calculated by simply inverting the previous one from phase space considerations (neglecting the lepton masses)

$$\sigma_{q+\bar{q} \rightarrow l^++l^-}(s) = \frac{1}{N_c^2} \frac{\sigma_{l^++l^- \rightarrow q+\bar{q}}(s)}{(1 - \frac{4m_q^2}{s})} \quad (16)$$

C. Lattice-based potentials for static quarks

As in [13] we use a potential extracted by parameterizing the Bielefeld data [15] on the effective static potentials (for details see [13]). These potentials are used

to solve the Schrodinger (or Klein Gordon) equation for different temperatures.

Another ingredient taken from lattice calculation is the quasiparticles masses. In [16] Petreczky et al. have shown that the masses of the quarks in the region of $1.5 - 3T_c$ stay roughly constant at a value of $Mq \approx 1GeV$. As in [12] we fix this value all the way up to T_c , being aware that the quasiparticles should become heavier close to the transition temperature.

It was also pointed out in [12] that in order to trigger the phase transition at $T = T_c$ the lowest $q\bar{q}$ bound state is required to become massless. The previous static potential is not enough to achieve this, and a quasi-local interaction induced by the *instanton-antiinstanton molecules* [12] [13] is needed. We will model this interaction by the following potential:

$$V_{inst} = \frac{U_0}{(r^2 + \rho^2)^3} \quad (17)$$

where $\rho = 1/3fm$ is the typical instanton size. The value U_0 is fixed at T_c by the requirement of the lowest level to be exactly massless (in the chiral limit). At higher temperature, the instantons are suppressed, which we model with the following damping factor

$$n(\rho, T) = n(\rho, T_c) \exp(-\frac{1}{3}(2N_c + N_f)(\pi\rho)^2(T^2 - T_c^2)) \quad (18)$$

Finally, the polarization of the instanton molecules along the (Euclidean) time direction leads to a distinction of the π and ρ channels, see discussion in [12]. To take this into account, the authors of [12] have multiplied the strength of the non-local interaction by a correction factor $U_0 \rightarrow U_0 F$ where for vectors $F = 0.7$.

III. RESULTS

First, let us explain our units. Since the effective mass of quark quasiparticle in the temperature interval considered is not known accurately, we use it as our basic energy unit. In plots twice this value appear as a threshold, to which we tentatively ascribe to it a particularly simple value $2M_q = 2GeV$: the reader should however be warned that this is a "GeV" in quotation marks, to be rescaled appropriately later when the value of quark effective masses in QGP will be better known.

A. A near-threshold region

Although the underlying potentials describing interaction between quasiparticles in the channels we consider are always attractive, due to presence of bound/virtual states the effective scattering amplitude is complex and its real part may even change sign. In particular, it is well known from quantum mechanics that since a scattering

amplitude changes sign at energy equal to the position of the level, an overall attractive potential can cause effective interaction of positive energy particles to be repulsive, if the level is close to zero. However this effect holds only for scattering states, or particles moved far away from the origin (where the potential is negligible). We however are interested in a shape of the annihilation signal: and thus we are only concerned about the wave function at the origin. Even in a case when a level approach zero, the effect of the attractive potential is only to increase the annihilation rate: there cannot be any opposite effect.

All of it can be studied in the simplest problem possible, that of a spherical potential well:

$$V = \begin{cases} 0, & (r > a) \\ -V_0, & (r < a) \end{cases} \quad (19)$$

Parametrizing $V_0 = \frac{(2n+1)^2 \pi^2}{4a^2 M}$ we find levels at threshold ($E = 0$) for n integer and n is the number of levels below threshold. It is straightforward now to solve the Green's function equation for this potential (15). Again, as we are only interested in the Green's function at the origin, we only need to calculate the s wave equation with the standard boundary conditions. The result of this simple calculation (in the limit $\Gamma \rightarrow 0^+$ is

$$\Im G_{E+i0^+}(0,0) = -\frac{1}{4} \frac{M\omega^2 k}{\pi((\omega^2 - k^2) \cos^2(\omega a) + k^2)} \quad (20)$$

And $\omega^2 = M(E + V_0)$, $k^2 = ME$. When n is not an integer, the Green's function close to zero behaves as $-\frac{1}{4} \frac{Mk}{\pi}$, that is, the value of the free Green's function. When n is integer, we have a level at $E = 0$ what leads to a divergence. We see then that the modifications at threshold come from the presence of bound states and virtual levels close to zero binding. In the case of coulomb potential, the finite value of this object at threshold is a consequence of the infinite number of states close to that energy.

We also observe that, according to (12), the cross section at any energy is bigger (or equal) than the free one, as correspond to an attractive potential. It is interesting to note that the oscillations at positive energy correspond to *virtual levels*, as the continuation of the denominator of 12 to imaginary values of k is the condition for bound states in the potential. The position of the maxima, then, reflects the position of these virtual levels.

Repeating the calculation that lead to (4) (see, for example, [5]) with the cross sections expressed in terms of the Green's function (12) we obtain the following expression

$$\Im \Pi_{em}(M) = -4 \Im G_{M-2m_q+i\Gamma_q}(0,0) \quad (21)$$

The calculation of the modification of the spectral density is now straight forward. The parametrization of lattice results plus the non local interaction described in the

previous section gives us a close expression for the interparticle potentials at different temperatures that we can use to solve (15). We do this numerically by following the numerical method of [21] based on finding two independent solutions of Schrodinger equations. We evaluate $\Im G_{M-2m_q+i\Gamma_q}(0,0)$ directly for "realistic" lattice-based potentials.

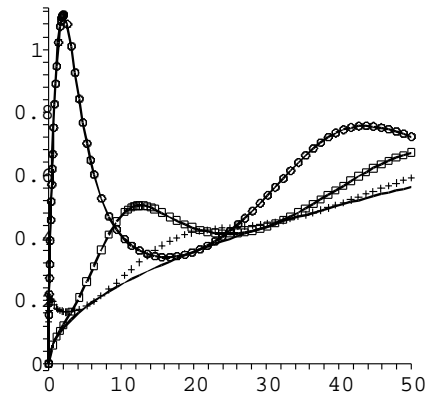


FIG. 3. $\Im G_{E+i0^+}(0,0)$ versus energy/mass for $a=1$ also in inverse mass units: Free case (solid), $n=0.01$ (cross), $n=0.5$ (box), $n=0.9$ (circle)

We still have to address the issue of the width. It is clear that the quasiparticles will have a thermal width in the equilibrated medium. Perturbative calculations for this quantity exist in the literature and to lowest order they are (at rest)

$$\Gamma = a(N, N_f) \frac{g_s^2 T C_F}{4\pi} \quad (22)$$

With $a(N, N_f) \approx 1.40$ for $N = 3$ and $N_f = 2$. For $T \approx (1-3)T_c$ and $\alpha_s \approx 0.5$ gives a width $\Gamma \approx 0.4-1 GeV$. These values of the width, comparable to the quasiparticle mass, are too big and would make very complicated to be able to extract a value for the masses from lattice data. Of course, there is no reason to believe that the perturbative expression makes sense for such a big value of α_s . That is why we follow a phenomenological approach, leaving the width as a free parameter and presenting our calculations for different values.

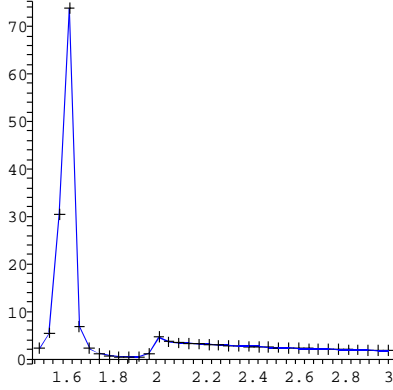


FIG. 4. Modification of the spectral density at T_c with respect to invariant mass in units of M_q . The peak at 1600 MeV corresponds to the ρ (non relativistic approximation). The peak at 2000 MeV reflects the threshold enhancement

We now move to present the results, starting with the warning. In figure 4 we show the modification of the spectral function, (the ratio (21) over (3)) at $T = T_c$ ($\Gamma = 10\text{MeV}$). One can see the threshold enhancement at 2 GeV and the peak around 1600 MeV corresponding to the bound state that should represent ρ at $T = T_c$. Although the potential we used has the same suppression of instanton molecules as in [12], instead of relativistic Klein Gordon equation used in that work we now use the nonrelativistic Schrodinger equation and thus found much less deeply bound state, with only about 400 MeV binding. (We checked that Klein Gordon equation with the same potential modified by for Schrodinger and by simulating the velocity-velocity term by effectively doubling the coupling [12] [13] indeed shifts ρ much lower, to about 600MeV , as found in that paper.)

Thus at $T \approx T_c$ the relativistic effects are very important. It means that one should either (i) develop fully relativistic theory of Green functions and dilepton rates, or (ii) restrict the discussion to the nonrelativistic domain at somewhat higher T not too close to T_c . In this work we only follow the latter option: the reader thus should be aware that our results should not be trusted close to T_c .

What we learned from these calculations is how the spectral density changes as the bound states become less and less bound until the system arrives to zero binding (zero binding point). In figure 5 we show the shape of the dilepton spectral density for different temperature ($1.2 T_c$, $1.4 T_c$, $1.7 T_c$, $3 T_c$). One can observe how exactly enhancement in the bound state and threshold region changes. The height of this enhancement depends on the proximity of the level; at $1.7 T_c$, where the bound level is close to threshold, we observe a big modification of the spectral function at 2GeV . Note that proximity of the level to threshold happens in rather wide T interval, roughly between $1.5 T_c$ to $2 T_c$ (the zero binding point [11]). Note also that the enhancement is still seen at tem-

peratures as high as $3 T_c$, when all bound states have already been melted.

We show in figure (6) the dependence of the modification factor with the width of the quasiparticles at a fixed temperature of $2 T_c$. The general features of the modification are the same. However, the extra enhancement due to the proximity to threshold is very sensitive to the width of the quasiparticles. But, we expect at least a factor 2 from the final calculation of the rates with the standard expression (3) for any reasonable value of the width.

B. Dilepton signal at RHIC

In this section we discuss the time-integrated dilepton production rates. We start with the QGP phase. We can observe an enhancement in the region close to 2 GeV. This is because in the whole region of temperatures accessible at RHIC we observe the bump in the cross section due to threshold effect. The contribution below threshold is strongly suppressed due to the mass effect. The value observed comes from the bound state moving from threshold till the value at T_c .

When we look at the contribution from the mixed phase, we can observe a significant threshold contribution. However the main contribution is given by the bound state at T_c . We remark again that this contribution should not be considered too seriously due to the relativistic character of the bound states.

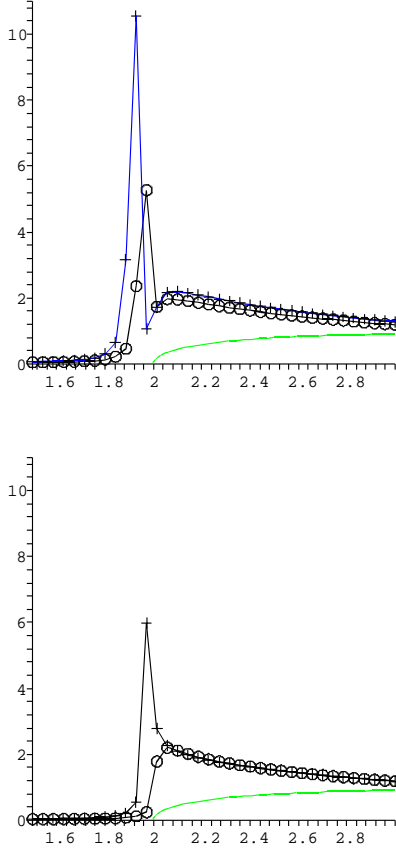


FIG. 5. Modification of the spectral density versus the invariant mass in M_q units for different temperatures: (a) 1.2 T_c (cross) and 1.4 T_c (circle), (b) 1.7 T_c (cross) and 3 T_c (circle) and the correction due to quark mass (line).

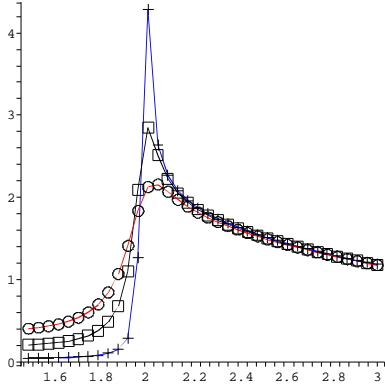


FIG. 6. Modification of the spectral density versus the invariant mass in M_q units. Dependence on the width (at $T = 2T_c$); $\Gamma = 10 MeV$ (cross), $\Gamma = 50 MeV$ (box), $\Gamma = 100 MeV$ (circle)

Finally we show the total modification of the production due to the QGP. We show the effect of the widths.

As the contribution of the mixed phase is much smaller than the QGP one, the effect of the bound states is not as prominent. At the same time the contribution from the threshold produces an enhancement that survives the time integration. Although both effects depend on the assume widths, they are present for values as big as $\Gamma = 100 MeV$. Thus, we do expect an observable modification of the spectrum in sQGP, relative to the wQGP calculation by Rapp [4].

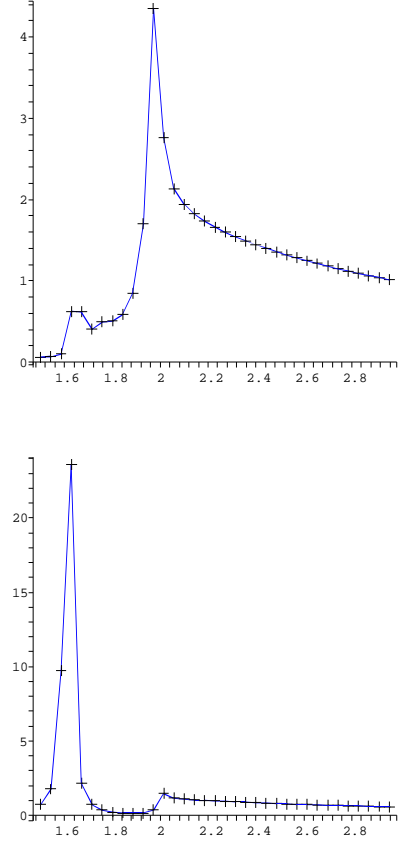


FIG. 7. The contribution of (a) the QGP phase and (b) the mixed phase at RHIC to total dilepton yield, normalized to the “standard rates” (note that both approach 1 at high masses). The calculation is done for $\Gamma = 10 MeV$, the invariant mass is given in units of M_q .

IV. TWO-PHOTON SIGNALS

At first glance, $\gamma\gamma$ spectroscopy looks even more promising than dileptons, since such decays can happen for wider range of channels – such as pseudoscalars, scalars and tensors.

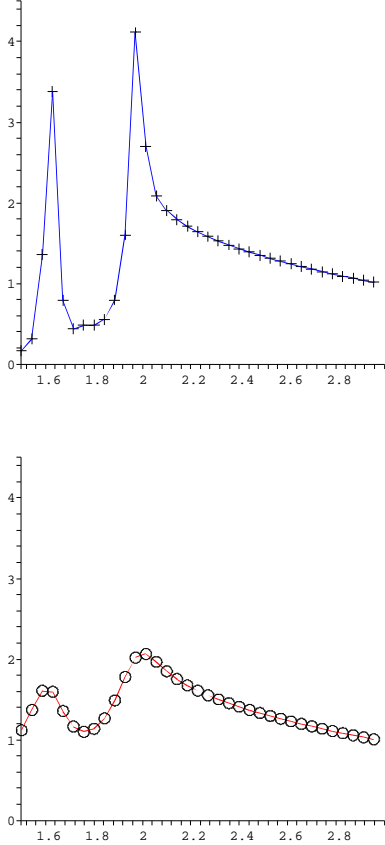


FIG. 8. The ratio of dilepton production from the QGP+mixed phase to “standard rate”, vs the invariant mass (in M_q units). The effect is shown for two widths (per quark), (a) $\Gamma = 10 \text{ MeV}$, (b) $\Gamma = 100 \text{ MeV}$

Pseudoscalars: In vacuum, as well as the hadronic phase $T < T_c$ the pseudoscalars π, η are Goldstone bosons, and their masses are protected by chiral symmetry, and thus if all quarks be massless they should remain zero. As it is well known, the near-SU(3)-singlet η' is not a Goldstone boson due to chiral anomaly and instantons, which explicitly violates the chiral $U(1)$ symmetry. A sketch of levels motion with T is shown in Fig.9. As T grows, the mixing between η' and η is expected to change as well, they start at $T = 0$ close to pure SU(3) singlet and octet, but above T_c they eventually rotate into purely light $\bar{u}u, \bar{d}d$ and strange $\bar{s}s$ states. This is related with the fact that the role of instanton-induced interaction diminishes with growing T , both because of reduced wave function at the origin of the bound states and because of instanton suppression by Debye screening.

For estimates of the rate we will need the corresponding electromagnetic widths, given by their total widths and diphoton branching ratios from the Particle Data Tables:

$$\Gamma_{\eta \rightarrow \gamma\gamma} = 1.18 \text{ keV} * .39 = .46 \text{ keV} \quad (23)$$

$$\Gamma_{\eta' \rightarrow \gamma\gamma} = .2 \text{ MeV} * 0.02 = 4 \text{ keV} \quad (24)$$

Scalars: As it is well known, the situation with scalar mesons is rather complex. The debates of whether the lightest scalars such as $f_0(600)$ (known formerly as σ of Gel-Mann-Levy sigma model) is a $\bar{q}q$ state go back decades, and some heavier scalars are now believed to be partly diquark-antidiquark states, and also mix with the scalar glueball. Not going into this discussion we only comment that above T_c (in the chiral limit) there must be degeneracy between pseudoscalar and scalar chiral partners of the pion and eta mesons. In other words, if quark chirality is conserved, there are identical states made of $\bar{q}_L q_R$ and $\bar{q}_R q_L$ quarks.

Tensors: $f_2(1270)$ is a famous example of a state seen in $\gamma\gamma$ collisions, its partial width is comparable to that of scalars and pseudoscalars, namely

$$\Gamma_{f \rightarrow \gamma\gamma} = 185 \text{ MeV} * 1.410^{-5} = 2.6 \text{ keV} \quad (25)$$

However at $T > T_c$ the situation is radically different: the calculations made in [13] show that all^{§§} P-wave states seem to be dissolving very close to T_c , and in fact the lattice-based effective potentials lead to a single s-wave bound states.

An estimate of the production rate may be done as follows

$$N_{\gamma\gamma} = \int \Gamma_{\gamma\gamma} n dtdV \quad (26)$$

where the integral is done over space-time occupied by sQGP. Using for estimate $t_{QGP} \sim 5 \text{ fm} \sim 1/(40 \text{ MeV})$ times gives small parameter $\Gamma t_{QGP} \sim (4 \text{ keV}/40 \text{ MeV}) \sim 10^{-4}$, originating ultimately from the electromagnetic coupling α_{em}^2 . The integral of density over volume $n dV$ is dominated by later stages and thus is approximately equal to the particle number produced at chemical freeze-out. Thus we conclude that for η, η' 2-photon signal the in-matter (modified) signals are about 4 orders of magnitude below those coming after freezeout.

If instead of $T \approx T_c$ we think now about the contribution to the time integral of the early times, at the vicinity of the zero binding point, the temperature is about twice higher but the mass of the state we would like to produce, with the energy $\approx 2M_q \approx 2 \text{ GeV}$ is also twice higher than the mass of the η' , resulting in about the same Boltzmann factor.

Good news about these rates is that there should be more states similar to π, η : adding scalars and states containing “plasminos” instead of quark quasiparticles leads to additional factor $2*4=8$ in the rate.

Unfortunately there are also small parameters involved, leading to further troubles for the $\gamma\gamma$ signal. The

^{§§}The only exception is the scalar glueball channel in which color Casimir is factor 9/4 stronger and P-wave state survives for a while. However glueball states are not relevant for electromagnetic probes anyway.

widths $\Gamma_{\gamma\gamma}$ of the pseudoscalar mesons in vacuum are proportional to f_π, f_η etc which (as one of the order parameters of chiral symmetry) must vanish at $T > T_c$ (in the chiral limit). What it means is simply the statement that those particles are bound state of $\bar{L}R$ or $\bar{R}L$ (where we mean left and right handedness of quarks) and in the chirally symmetric QGP phase L and R are like different quark flavors, which simply cannot annihilate each other as they are not antiparticle of each other. In order that to become possible, one should admit chirality flip in the process, or the first power of a current quark in the amplitude, resulting in additional suppression factor

$$\frac{\Gamma_{\gamma\gamma}(T > T_c)}{\Gamma_{\gamma\gamma}(T < T_c)} \sim \left(\frac{m_s}{M}\right)^2 \quad (27)$$

which reduces the effect by about an order of magnitude for strange quarks (e.g. in η, η') and much more so for the pion.

Although the authors are not qualified to tell what exactly the limits of experimental detection of this effect is, it looks to be rather difficult to measure these effects.

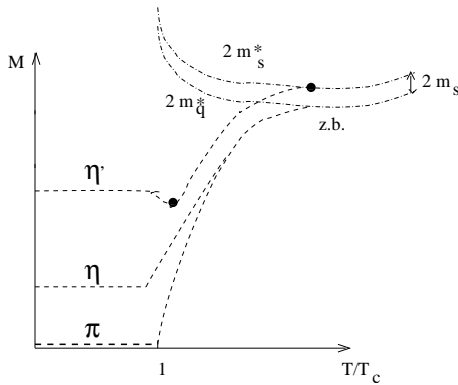


FIG. 9. Schematic T -dependence of the masses of $\bar{q}q$ pseudoscalar states. Two dash-dotted lines show a behavior of twice the quark quasiparticle mass, for light and strange quarks, respectively. Two black dots indicate places where $\gamma\gamma$ signal may be observable.

V. SUMMARY AND DISCUSSION

We have proposed in this work new direction of dilepton experiments, namely looking for the bound vector $\bar{q}q$ states and threshold enhancement in the QGP domain. We in particular identified 2 regions of the dilepton invariant mass as most promising, corresponding to two endpoints of the sQGP domain.

In a nonrelativistic approach, we worked out a numerical method for the determination of the Green function and annihilation rate, using all states, bound and unbound. We used realistic interaction and have studied in detail the shape of spectral density as a bound level approach a threshold.

We have also performed realistic averaging over an expanding fireball, using parameters for RHIC, and demon-

strate that this averaging does not eliminate the contribution of the peaks near two ends of the sQGP region. The actual observability of states still depend on the issue of the width of these states. We have decided at this point to leave this issue open for further studies. The reason for that is the rather uncertain theory of sQGP and its near-perfect liquid properties. For the first investigations of the “photo-effect”-like reactions with splitting of the binary bound states see [25]. Lattice studies do see these peaks, which is encouraging, but the maximal entropy method they use in [14] was not studied enough to tell how accurately the widths can really be estimated by it.

We pointed out that in principle a dilepton study can be complemented by a $\gamma\gamma$ one, for scalars and pseudoscalars from sQGP. Interesting signals can be expected around T_c and the same threshold phenomena near the endpoint as for dileptons. However, much higher background makes it more difficult to do.

Acknowledgments. We thank G. Brown for useful discussions at the early stages of this work, and we are happy to thank V. Zakharov for an interesting discussion. This work was partially supported by the US-DOE grants DE-FG02-88ER40388 and DE-FG03-97ER4014.

-
- [1] E. V. Shuryak, Phys. Lett. **B78** (1978) 150, Yadernaya Fizika (Sov.J. of Nucl. Physics) **28** (1978) 796. Phys.Rep. **61** (1980) 71.
 - [2] R. Rapp, E. V. Shuryak, Phys. Lett. B **473**, 13 (2000)
 - [3] B. Kämpfer, K. Gallmeister, O.P. Pavlenko, hep-ph/0102192, Phys. Lett. B **473** (2000) 20.
 - [4] R. Rapp, Thermal lepton production in heavy-ion collisions, nucl-th/0204003, see also hep-ph/0201101
 - [5] R. Rapp and J. Wambach, collisions,” Adv. Nucl. Phys. **25**, 1 (2000) [hep-ph/9909229].
 - [6] G. Q. Li, G. E. Brown and C. M. Ko, Nucl. Phys. A **630**, 563 (1998) [nucl-th/9706022].
 - [7] E. V. Shuryak, Nucl. Phys. A **533**, 761 (1991).
 - [8] E. V. Shuryak and G. E. Brown, Nucl. Phys. A **717**, 322 (2003) [arXiv:hep-ph/0211119].
 - [9] P. Fachini, Acta Phys. Polon. B **35**, 183 (2004) [arXiv:nucl-ex/0311023].
 - [10] K. Adcox et al., Phys. Rev. Lett **88**, 192303 (2002). [arXiv:nucl-ex/0202002].
 - [11] E.V. Shuryak and I. Zahed, hep-ph/0307267, Phys.Rev.C, in press.
 - [12] G. E. Brown, C. H. Lee, M. Rho and E. Shuryak, hep-ph/0312175.
 - [13] E. V. Shuryak and I. Zahed, arXiv:hep-ph/0403127. submitted to Phys.Rev.D.
 - [14] S. Datta, F. Karsch, P. Petreczky and I. Wetzorke, hep-lat/0403017; M. Asakawa and T. Hatsuda, hep-lat/0308034.
 - [15] O. Kaczmarek, S. Ejiri, F. Karsch, E. Laermann and F. Zantow, hep-lat/0312015.

- [16] P. Petreczky, F. Karsch, E. Laermann, S. Stickan, I. Wet-
zorke, Nucl. Phys. Proc. Suppl. **106** (2002) 513.
- [17] O. Kaczmarek, S. Ejiri, F. Karsch, E. Laermann and F.
Zantow, **hep-lat/0312015**.
- [18] E.V. Shuryak and I. Zahed, Phys. Rev. **D69** (2004)
014011. [arXiv:hep-th/0308073].
- [19] B.Gelman, E.Shuryak and I.Zahed, Viscosity of strongly
coupled atomic systems, in progress.
- [20] V. S. Fadin and V. A. Khoze, Threshold Sov. J. Nucl.
Phys. **48**, 309 (1988) [Yad. Fiz. **48**, 487 (1988)].
- [21] M. J. Strassler and M. E. Peskin, Phys. Rev. D **43**, 1500
(1991).
- [22] M. A. Shifman, A. I. Vainshtein and V. I. Zakharov,
Nucl.Phys. **B147**, 385 (1979).
- [23] M.A. Shifman, in *Continuous Advances in QCD*, Ed. A.
Smilga (World Scientific, Singapore 1994), p. 249 [hep-
ph/9405246]. B. Chibisov, R.D. Dikeman, M. Shifman
and N. Uraltsev, *Int. J. Mod. Phys. A* **12** 2075 (1997)
- [24] J. I. Kapusta and E. V. Shuryak, Phys. Rev. D **49**, 4694
(1994) [hep-ph/9312245].
- [25] E. V. Shuryak and I. Zahed, Ionization of binary bound
states in a strongly coupled quark-gluon plasma, hep-
ph/0406100.